

Emission of Energetic Secondary Electrons Produced by 1.3-Mev Electron Bombardment*

R. A. SHATAS, J. F. MARSHALL, AND M. A. POMERANTZ

Bartol Research Foundation of The Franklin Institute, Swarthmore, Pennsylvania

(Received May 6, 1954)

The emission of energetic secondary electrons (delta rays or knock-on electrons) produced by 1.3-Mev primaries which penetrate thin targets with negligible mean energy loss has been investigated. These have previously not been observable in the customary thick-target experiments because of the inherent impossibility of distinguishing between true secondaries and reflected primaries which have suffered large energy losses. The present arrangement does not record back-scattered primaries, but only emitted electrons. The delta ray yields from various targets (Al, Ni, Au, Ag, Cu, C) ranging in thickness from 5×10^{-6} to 10^{-2} in. have been measured. The determinations of I_s/I_P vary between 0.3 percent and 2.1 percent independent of surface treatment, and there is only a small dependence of the yield upon target material for an equivalent thickness expressed in mg cm^{-2} . For 45.8 mg cm^{-2} Ni, the delta ray yield is 2.08 ± 0.15 percent. This may be compared with 1.48 ± 0.25 percent, the yield of low-energy secondaries as measured with the cleanest surface attainable in the demountable experimental tube.

I. INTRODUCTION

ALTHOUGH secondary emission from solids bombarded by electrons having energies below several thousand ev has been the subject of considerable investigation, the advantages of extending the observations to high primary energies have remained generally unrecognized. Sources of electrons in the Mev region have been available for many years, and numerous studies of electron scattering have been conducted. Nevertheless, the only previous secondary emission measurements have been those in the range from 30 kev to 340 kev obtained by Trump and Van de Graaff¹ with the electrostatic generator in the course of experiments directed primarily at investigating the mechanisms of voltage breakdown in high vacuum, and from 18 kev to 1.4 Mev by Miller and Porter² with the linear accelerator.

The conventional arrangement for measuring the yield of secondary electrons involves a thick target in which the primary is completely absorbed. When the bombarding energy is low, the description of the phenomenon of secondary emission comprises essentially four processes, some of which are not particularly amenable to theoretical analysis. These are: (1) the primary interaction, (2) the primary energy loss, (3) the escape of secondaries, and (4) integration of the first three steps over the range of the primary. By invoking a combination of very high primary energy and targets which are sufficiently thin to permit the bombarding electrons to pass through with negligible scattering and energy loss, a significant simplification of the theoretical treatment results. For this reason, and in order to study certain other aspects of secondary electron emission, a program of experiments was undertaken utilizing the multiple-cavity linear accelerator

as the source of a 1.3-Mev electron beam. In contrast with the methods employed previously, the present techniques have permitted the direct observation of energetic secondary electrons, long familiar to cosmic ray investigators as *knock-on electrons* or *delta rays*.

II. EXPERIMENTAL PROCEDURE

A. Method

The electrons leaving a bombarded target can be ascribed to three different mechanisms. Some of the primary electrons are directly reflected, whereas others are scattered with some loss of energy. Finally, secondary electrons are emitted by the target as a consequence of interactions between the primary electrons and the electrons in the solid. In the usual experimental arrangement, which is illustrated schematically in Fig. 1(a), it is impossible to distinguish between true secondaries and back-scattered primaries which have suffered large energy losses. In this case, the target current, $I_P - I_S$, is the difference between the total primary current and the current of secondary electrons plus back-scattered primaries which do not return to the

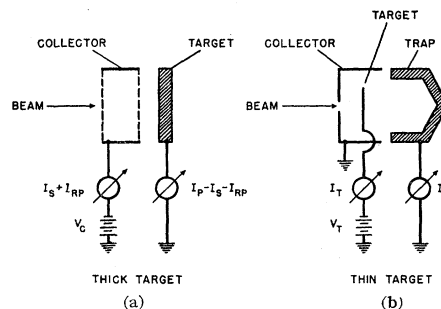


FIG. 1(a). Conventional arrangement for measuring secondary electron emission from thick targets. It is impossible to distinguish between energetic secondaries and back-scattered primaries in this case. (b). Arrangement for measuring secondary electron emission from thin targets through which the primaries pass with negligible energy loss. Primaries scattered from the target are not recorded.

* Assisted by the Office of Ordnance Research and the U. S. Office of Naval Research.

¹ J. G. Trump and R. J. Van de Graaff, J. Appl. Phys. **18**, 327 (1947); Phys. Rev. **75**, 44 (1949).

² B. L. Miller and W. C. Porter, Phys. Rev. **85**, 391 (1952).

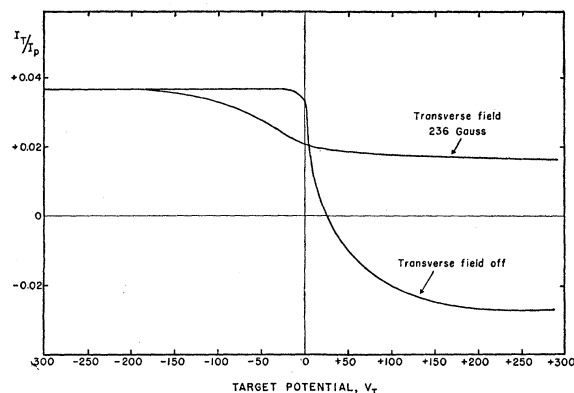


FIG. 2. Dependence of I_T/I_P upon V_T [see Fig. 1(b)] with and without a transverse magnetic field. The ratio is defined as positive when there is a net emission of electrons from the target.

target. The collector current is composed of both secondary electrons leaving the target, I_S , and primaries scattered from the target, I_{RP} . The classification in terms of secondaries and scattered or reflected primaries is made on the basis of the energy distribution of the collected electrons, obtained by applying retarding potentials, $-V_C$, to the collector with respect to the target. Collected electrons which can overcome some rather arbitrarily-assigned retarding potential are then regarded as scattered and reflected primaries, whereas the electrons of lower energies are designated as true secondaries. Thus, high-energy secondaries and scattered primaries are indistinguishable, and the contribution of the former to the total yield is, in fact, assumed to be negligible.

In the present arrangement, shown in Fig. 1(b), the scattered primaries are not recorded. When the potential of the target is positive with respect to the surroundings, the target current,³ I_T , represents the difference between those secondaries which have sufficient energy to overcome the retarding potential, V_T , and the secondaries from the surroundings (trap and collector electrodes) which are attracted to the target. The primary beam penetrates the target, and is observed as the trap current,⁴ I_P , the magnitude of which

³ Contributions to I_T from sources other than low energy secondary electrons are negligible. Back-scattered primaries and delta rays leaving the graphite trap amount to less than 3 percent of the incident beam (see reference 1) and only a fraction ($\approx \frac{1}{4}$) of these strike the target. Inasmuch as their energies are, in general, high compared with that necessary to penetrate the thickest target employed, their effect upon I_T is not observable. Because of the phenomenon of delta-ray emission, the effect of stopped primaries cannot be determined experimentally. However, theoretical computations based upon Yang's expression for the distribution in path lengths of electrons penetrating thin foils [C. N. Yang, Phys. Rev. 84, 599 (1951)] reveal that in the most extreme case from this point of view ($45.8 \text{ mg cm}^{-2} \text{ Ni}$) only 0.05 percent of the emergent primaries traverse paths exceeding 1.5 times the thickness of the foil. Since the range of the primaries is 15 times that of this particular target, obviously only a minute fraction of the primaries will stop.

⁴ Although I_P actually represents the incident primary current minus back-scattered primaries and secondaries escaping from the trap electrode, the contributions of the latter are negligible.

is essentially unaffected by the presence of the thin targets utilized in the present experiments. The secondaries from the surroundings can be prevented from reaching the target by the application of a transverse magnetic field of appropriate magnitude in the vicinity of the target, thereby permitting the determination of the delta ray yield.

The effect is revealed in Fig. 2, which shows the dependence of the ratio,⁵ I_T/I_P , upon target potential, V_T , with a transverse magnetic field either on or off. With no magnetic field, all of the secondaries leave the target when V_T is negative. In this case, low-energy secondaries from the surroundings are repelled by the target, although high-energy secondaries may be collected. However, when the target potential is between -15 v and zero, all extraneous low-energy secondaries are not retarded, and those which strike the target cause the net target current to decrease. When V_T is sufficiently positive, a net collection of electrons by the target occurs, since the low-energy secondaries from the surroundings are now attracted, and the yield becomes negative. However, the application of a transverse magnetic field prevents the stray electrons from reaching the target, and a net emission is manifested by the positive yield.

This provides a lower limit for the delta-ray yield, since both imperfect protection of the target from extraneous electrons and the return of emitted delta rays to the target tend to reduce the net target current. In practice, the measured value probably coincides with the actual value within the experimental uncertainty.

B. Tube Design

The arrangement of the electrodes in the demountable experimental tube is shown in Fig. 3. The tube is

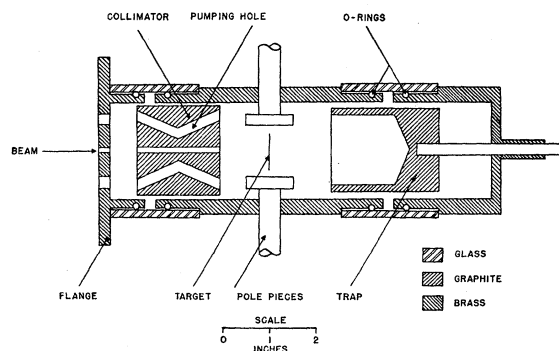


FIG. 3. Cross-sectional view of experimental tube utilized for determination of secondary electron yields.

The error in the yields arising from neglect of back-scattered primaries and secondaries ($<0.03I_P$) is less than other experimental uncertainties.

⁵ The ratio I_T/I_P is defined as positive when the sense of the current I_T corresponds to a net emission of electrons from the target, and negative when the number of electrons emitted is less than the number collected from other sources, per primary electron.

attached to a magnetic spectrum analyzer by means of a flange with an O-ring gasket at the output end of the linear accelerator.

The graphite collimator defines the size of the primary beam, which is approximately 6 mm in diameter at the target. The eccentric pumping holes provide adequate pumping speed without the introduction into the target region of the copious background of stray electrons from the analyzer.

The target is supported by a rod equipped with a sliding O-ring gasket arrangement (not illustrated) which permits positioning the 1-in. \times 1 $\frac{1}{4}$ -in. foil in or out of the path of the beam by remote control. The graphite trap which collects the primary electrons after they have penetrated the target can also be moved in vacuum to facilitate observations of any possible dependence of the results upon geometrical factors. In order to preclude the influence of ionization currents generated by the intense x-ray background, coaxial leads (not shown in Fig. 3) insulated from the brass envelope, are introduced through vacuum seals.

C. Linear Accelerator and Auxiliary Apparatus

The essential features of the four-cavity linear accelerator utilized in these experiments have been described previously.⁶ Several modifications have produced a high degree of stability in operation, and the maximum attainable output current has been increased to peak values of 60 ma at 1.3–1.5 Mev by removal of the buncher cavity and improvements in the electron injection system. In the present measurements, the targets were generally bombarded by rectangular one microsecond pulses of primary electrons at a repetition rate of 20 pulses per second and pulse height 0.05–1.0 ma. The energy spectrum, determined by the geometry of the analyzer, is triangular with a half-width of 7 percent, corresponding to 94 kev at 1.35 Mev.

Trap and target currents are measured simultaneously by a pair of two-stage negative-feedback dc amplifiers⁷ with integrating networks in the input. The maximum sensitivity is 10⁻¹² amp per division, and the variation in the calibration of the electronic meters is less than 1 percent.

D. Determination of Delta Ray Yields

Figure 4 represents the series of observations comprising a typical delta ray yield determination. A potential as low as +18 v applied to the target with respect to its surroundings is sufficient to impede the escape of the low-energy secondaries produced in the target. However, in the absence of a transverse magnetic field, low-energy secondaries emitted by the auxiliary electrodes are collected by the target, as a result of which a small net negative I_T/I_P is measured. When the transverse field is applied, stray low-energy second-

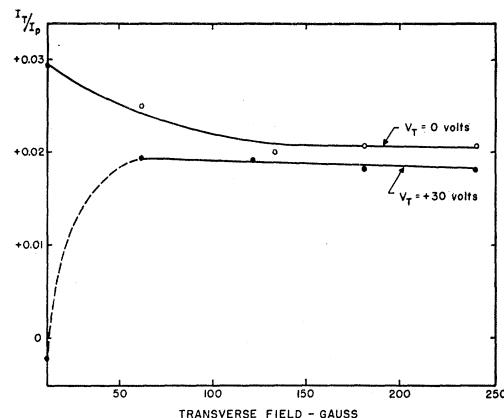


FIG. 4. Typical series of observations of delta-ray yield. With $V_T > 18$ v, I_T/I_P is measured as a function of the transverse magnetic field strength. Plateau values represent I_δ/I_P .

aries are deflected away from the target, and with the field strength of appropriate magnitude, the target current is comprised primarily of electrons emitted by the target. I_T/I_P then remains constant over a "plateau" region of magnetic field strength. This reveals that a negligible contribution is attributable to extraneous effects. As confirmed by direct observation with a fluorescent screen placed at the position normally occupied by the trap, the primary beam is deflected considerably, and hence suffers appreciable scattering while traversing the collimator, when the field intensity exceeds a maximum value, which with the present arrangement is 240 gauss.

The delta ray yield of a particular target is determined from the average of at least eight individual measurements, with two different target voltages, spanning the magnetic field strength plateau. The dependence upon V_T , ($V_T > +18$ v) is negligible.

E. Targets

Various metals (Al, Ni, Au, Ag, Cu) commercially available in foil, leaf, or sheet form, ranging in thickness from 5×10^{-6} in. (Au) to 10^{-2} in. (Al) were employed as targets. Carbon targets were prepared by grinding the faces of a thin section sliced from a 1-in. diameter graphite rod.

In contrast with the conditions which prevail in measurements of low-energy secondary electrons, it is not necessary to exercise the customary precautions regarding surface cleanliness in view of the high energy with which the delta rays emerge.

III. RESULTS

All of the determinations of delta-ray yield are summarized in Fig. 5, where I_δ/I_P is plotted as a function of target thickness expressed in mg cm⁻². The standard deviation of each point is approximately ± 10 percent of the indicated value. The experimental uncertainty is governed by fluctuations of the primary

⁶ B. L. Miller, Rev. Sci. Instr. 23, 401 (1952).

⁷ S. Roberts, Rev. Sci. Instr. 10, 181 (1939).

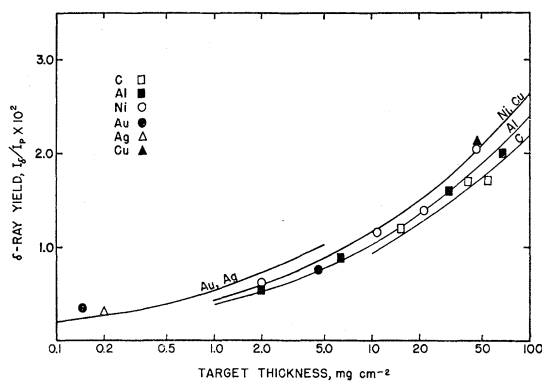


FIG. 5. Dependence of delta-ray yield from various materials upon target thickness. The solid curves represent the theoretical predictions discussed in Sec. IV.

beam. Data obtained with a preliminary experimental tube having different dimensions from those indicated in Fig. 3 were in satisfactory accord with these results. Detailed comparison of total yields, including low-energy secondaries, was not attempted because of the dependence of the latter upon surface conditions. However, it is of interest to note the relative magnitudes of the yields of low- and high-energy secondaries from a typical target.

Although the delta-ray yield was independent of surface treatment in all cases, the *total* yield invariably decreased when the target was degassed by electron bombardment from an adjacent filament in the experimental tube immediately prior to the measurement. The minimum low-energy yield from 45.8 mg cm^{-2} Ni subjected to the maximum practicable heating was 1.48 ± 0.25 percent, a value which is presumably higher than that characteristic of an extremely clean specimen. The corresponding delta-ray yield is 2.08 ± 0.15 percent. Measurements of the yield of low-energy secondaries are now under way with sealed-off tubes processed in accordance with the procedures requisite for insuring the cleanliness of the target surfaces.

IV. THEORETICAL DISCUSSION

On the basis of a model involving several simplifying approximations, the delta-ray yield expected theoretically from a target of specified atomic number and thickness may be computed. The assumptions are: (a) the electrons in the target can be treated as unbound; (b) the delta-ray energies are much lower than the energy of the primary; and (c) a secondary created at a distance x from the surface of the target will emerge if its residual range is greater than x .

Under these conditions, the delta-ray yield (δ) is given by

$$\delta = \int_0^l f(E) dx, \quad (1)$$

where $f(E)$ is the number of secondaries produced per

unit path of the primary, with energy greater than E , the minimum energy necessary for escape from depth $(l-x)$, and l is the thickness of the target. Assuming the rate of energy loss of the secondaries to be given by

$$dE/dx = -\psi(E) \quad (2)$$

and changing the variable of integration in Eq. (1) from x to E , we obtain

$$\delta = \int_0^{E_l} \frac{f(E)}{\psi(E)} dE, \quad (3)$$

where E_l is the energy of an electron whose range is equal to l , and is obtained from

$$l = \int_0^{E_l} \frac{dE}{\psi(E)}. \quad (4)$$

The rate of production of internal secondaries may be obtained either from Møller's expression⁸ for the production of knock-on electrons, or from a purely classical calculation. Both yield

$$f(E) = C\mu/E. \quad (5)$$

Here, $\mu = mc^2$, the rest energy of the electron, and

$$C = 2\pi N_0 e^2 Z/A = 0.3(Z/A) \text{ g}^{-1} \text{ cm}^2,$$

where N_0 is Avogadro's number, Z and A are the charge and mass numbers of the target material, and $r_0 = e^2/\mu$ is the classical radius of the electron.

The rate of energy loss is given by the Bethe-Bloch expression,

$$\psi(E) = (C\mu^2/E) \ln(2E/I) \text{ ev g}^{-1} \text{ cm}^2. \quad (6)$$

(Relativistic effects are unimportant in the present case.) Here, as is customary, I is assumed to be proportional to the atomic number of the target material, $I = aZ$. The final results are found to be extremely insensitive to the choice of the constant of proportionality, and for purposes of calculation, a is taken to be 11.5 ev.⁹

Substituting Eqs. (5) and (6) in Eq. (3), one obtains

$$\delta = \frac{I}{2\mu} \bar{E}i \left(\ln \frac{2E_l}{I} \right), \quad (7)$$

where

$$\bar{E}i(x) = \int_{-\infty}^x \frac{e^{-t}}{t} dt$$

and Eq. (4) becomes

$$l = \frac{I^2}{4C\mu^2} \bar{E}i \left(2 \ln \frac{2E_l}{I} \right). \quad (8)$$

Solving Eq. (8) for $\ln(2E_l/I)$ and substituting in Eq.

⁸ C. Møller, Ann. Physik 14, 531 (1932).

⁹ R. R. Wilson, Phys. Rev. 60, 749 (1941).

(7), one then obtains the delta-ray yield as a function of the thickness and atomic number of the target.

From an analysis similar to that already outlined, one can determine the energy distribution of the emergent secondaries, and it is found that almost all of them have energies between 10 and 100 kev.¹⁰ Consequently, assumption (b) is valid, as is (a) for all but the most tightly-bound target electrons. Assumption (c) is not so well justified, since the path of an emerging secondary is in general longer than the distance from its point of origin to the surface, and the computed yields are consequently too high by about a factor of two. The ratio of the computed to the experimentally-

¹⁰ A lower limit to the delta-ray energies has been determined by an independent method of observing the energy distribution of the low-energy secondary electrons, and no current of delta rays with energies less than 2 kev has been detected [Shatas, Marshall, and Pomerantz, *Phys. Rev.* **94**, 757 (1954)].

determined yield is, however, substantially the same in all cases, indicating that the dependence of the delta ray yield on the thickness and atomic number of the target is correctly given by Eq. (7).

The computed yields normalized to fit the experimental value for 46 mg cm⁻² Ni are plotted in Fig. 5. Theory and experiment are in agreement within the experimental uncertainties, except for the case of 5 mg cm⁻² Au. This discrepancy may be caused by the fact that the scattering of the secondaries has not been taken into account in the theory. This effect would be more pronounced in a high-*Z* material such as gold.

ACKNOWLEDGMENT

The authors wish to acknowledge the assistance of Arthur E. Smith in the experimental program.

Hall Effect in Bismuth at Low Temperatures*

J. M. REYNOLDS, H. W. HEMSTREET, T. E. LEINHARDT, AND D. D. TRIANTOS

Physics Department, Louisiana State University, Baton Rouge, Louisiana

(Received July 30, 1954)

The dc Hall effect in bismuth has been investigated over a range of fields from 0 to 8000 gauss and at temperatures in the liquid helium region. It is observed that the Hall effect oscillates in a manner which is periodic in H^{-1} and that this period is independent of temperature. The dependence of the amplitude of the oscillations on field and temperature is of the general form given by the theoretical work of Grimsal and Levinger.

AT low temperatures the magnetic susceptibility of bismuth and many other metals shows oscillations which are periodic in the reciprocal of the magnetic field intensity.¹⁻³ At high fields such oscillations occur to a smaller extent in the magnetoresistance.⁴ The Peierls,⁵ Blackman,⁶ and Landau⁷ theory relates the oscillations of the de Haas-van Alphen effect to the Larmor precessions of the conduction electrons and to the quantization of this motion in the plane perpendicular to the magnetic field. As this precession gives rise to the Hall effect, it is not surprising that the Hall effect in bismuth is also periodic in $1/H$.⁸ Grimsal and Levinger⁹ have re-

cently obtained a formula for the periodic part of the Hall effect in bismuth, based on Blackman's formulation⁶ of the theory of the de Haas-van Alphen effect. The data reported here are interpreted in terms of Grimsal and Levinger's formulation.

EXPERIMENTAL

The single crystals were grown in vacuum by the Bridgman method, from Johnson, Matthey bismuth (Johnson, Matthey & Co., Ltd., London). Crystal Bi-1, reported on earlier,⁸ was in the form of a right parallelepiped of dimensions 25.5 by 7.5 by 0.88 mm. The orientation of its crystallographic axes were such that when mounted in the flask the current passed parallel to a binary axis and the magnetic field was at an angle of 25° with the trigonal axis.

In order to allow measurements to be made on one crystal, both with the field parallel and with it perpendicular to the trigonal axis, a crystal (Bi-4) was prepared which was more nearly cubical in shape (6.7×5.2×5.2 mm), with one pair of faces perpendicular to the trigonal axis, another pair perpendicular to a binary axis, and the third pair of faces parallel to the plane of

* Supported by the National Science Foundation.

¹ W. J. de Haas and P. M. van Alphen, *Leiden Comm. No. 212a* (1930) and No. **220d** (1932).

² D. Schoenberg, *Proc. Roy. Soc. (London)* **A170**, 341 (1939).

³ D. Schoenberg, *Trans. Roy. Soc. (London)* **A245**, 1 (1952).

⁴ P. B. Alers and R. T. Webber, *Phys. Rev.* **91**, 1060 (1953).

⁵ R. Peierls, *Z. Physik* **80**, 763 (1933).

⁶ M. Blackman, *Proc. Roy. Soc. (London)* **A166**, 1 (1938).

⁷ L. D. Landau, see Appendix to reference 2.

⁸ Reynolds, Leinhardt, and Hemstreet, *Phys. Rev.* **93**, 247 (1954).

⁹ J. S. Levinger and E. G. Grimsal, *Phys. Rev.* **94**, 772(A) (1954); and E. G. Grimsal, Thesis, Louisiana State University (1954) (Unpublished—copies available from L. S. U. Physics Department.)